Inorg. Chem. **2006**, *45*, 7032–7034

Chiral Molecule-Based Ferrimagnets with Helical Structures

He-Rui Wen, Cai-Feng Wang, Yi-Zhi Li, Jing-Lin Zuo,* You Song,* and Xiao-Zeng You

Coordination Chemistry Institute and the State Key Laboratory of Coordination Chemistry, Nanjing University, Nanjing 210093, People's Republic of China

Received March 18, 2006

Two enantiopure one-dimensional complexes with helical structures, $[Mn_3((R,R)\text{-Salcy})_3(H_2O)_2Fe(CN)_6\cdot 2H_2O]_n$ (**1**) and $[Mn_3((S,S)\text{-Salcy})_3(H_2O)_2Fe(CN)_6\cdot 2H_2O]_n$ (**2**) [Salcy = *N*,*N*′-(1,2-cyclohexanediylethylene)bis(salicylideneiminato) dianion], have been synthesized and characterized. Magnetic studies show that both complexes are ferrimagnets with the magnetic transition temperature at 3 K.

Since Rikken and Raupach first experimentally observed the weak magnetochiral dichroism (MChD) effect,[1] the investigation of chiral magnets combining magnetism and optical activity has become an active research topic because of its important potential application as multifunctional materials, such as switching functions.[2] Theoretically, fully chiral molecule-based magnets may exhibit a strong MChD effect. The design and synthesis of chiral molecule-based magnets is currently a challenging target because the chirality must be controlled in the molecular structure as well as in the entire crystal structure. To date, the introduction of magnetic order and natural optical activity at a molecular level is novel and there are only a few examples of molecule-based chiral magnets.[2−4]

Cyanide is an efficient and versatile mediator for magnetic coupling. The cyano-bridged bimetallic assemblies have been widely studied because of their rich magnetic behavior, including high-T_c magnetism, photo- and electromagnetism, and single-molecule or single-chain magnetism.[5] Recently, a strategy of using hexacyanometallic anions as bridging units to magnetic metal ions partially blocked by chiral diamine ligands was used to prepare chiral ferromagnetic compounds.[4] Miyasaka et al. have prepared a series of cyano-bridged complexes derived from the reaction of manganese(III) Schiff base complexes and hexacyanometallic anions.[6] To develop new chiral magnets, we focused our attention on chiral bimetallic systems with cyanometallic anions and enantiopure Schiff base complexes. Herein, we report the syntheses and optical and magnetic properties of two new cyano-bridged heterobimetallic chiral ferrimagnets with helical structures, $[Mn_3((R,R)\text{-Salcy})_3(H_2O)_2Fe(CN)_6\cdot 2H_2O]_n$ (**1**) and $[Mn_3((S,S)\text{-Salcy})_3(H_2O)_2Fe(CN)_6\cdot 2H_2O]_n$ (**2**) [Salcy = *N*,*N*′-(1,2-cyclohexanediylethylene)bis(salicylideneiminato) dianion].

Compounds **1** and **2**[7] were obtained as brown-black needle-shaped crystals by the reaction of a solution of $[Bu_4N]_3[Fe(CN)_6]$ and $[Mn((R,R)\text{-Salcy})(H_2O)_2]ClO_4$ or $[Mn((S,S)\text{-Salcy})(H_2O)_2]ClO_4$ in a 1:3 molar ratio in acetonitrile under room temperature. **1** and **2** are enantiomers and crystallized in the chiral space group $P2_12_12_1$; no detailed structural

* To whom correspondence should be addressed. E-mail: zuojl@nju.edu.cn (J.-L.Z.), yousong@nju.edu.cn (Y.S.).

(1) Rikken, G. L. J. A.; Raupach, E. *Nature* **1997**, *390*, 493−494.

(2) (a) Hernández-Molina, M.; Lloret, F.; Ruiz-Pérez, C.; Julve, M. *Inorg. Chem.* **1998**, *37*, 4131−4135. (b) Kumagai, H.; Inoue, K. *Angew. Chem., Int. Ed. Engl.* **1999**, *38*, 1601−1603. (c) Andrés, R.; Brissard, M.; Gruselle, M.; Train, C.; Vaissermann, J.; Malézieux, B.; Jamet, J.-P.; Verdaguer, M. *Inorg. Chem.* **2001**, *40*, 4633−4640. (d) Coronado, E.; Galán-Mascarós, J. R.; Gómez-García, C. J.; Martinez-Agudo, J. M. *Inorg. Chem.* **2001**, *40*, 113−120. (e) Minguet, M.; Luneau, D.; Lhotel, E.; Villar, V.; Paulsen, C.; Amabilino, D. B.; Veciana, J. *Angew. Chem., Int. Ed.* **2002**, *41*, 586−589.

(3) (a) Coronado, E.; Gómez-García, C. J.; Nuez, A.; Romero, F. M.; Waerenborgh, J. C. *Chem. Mater.* **2006**, *18*, 2670−2681. (b) Coronado, E.; Galán-Mascarós, J. R.; Gómez-García, C. J.; Murcia-Martínez, A. *Chem.—Eur. J.* **2006**, *12*, 3484−3492.

(4) (a) Inoue, K.; Imai, H.; Ghalsasi, P. S.; Kikuchi, K.; Ohba, M.; Ôkawa, H.; Yakhmi, J. V. *Angew. Chem., Int. Ed.* **2001**, *40*, 4242−4245. (b) Coronado, E.; Gómez-García, C. J.; Nuez, A.; Romero, F. M.; Rusanov, E.; Stoeckli-Evans, H. *Inorg. Chem.* **2002**, *41*, 4615−4617. (c) Inoue, K.; Kikuchi, K.; Ohba, M.; Ôkawa, H. *Angew. Chem., Int. Ed.* **2003**, *42*, 4810−4813. (d) Imai, H.; Inoue, K.; Kikuchi, K.; Yoshida, Y.; Ito, M.; Sunahara, T.; Onaka, S. *Angew. Chem., Int. Ed.* **2004**, *43*, 5618−5621.

(5) (a) Sato, O.; Iyoda, T.; Fujishima, A.; Hashimoto, K. *Science* **1996**, *271*, 49−51. (b) Holmes, S. M.; Girolami, G. S. *J. Am. Chem. Soc.* **1999**, *121*, 5593−5594. (c) Hatlevik, Ø.; Buschman, W. E.; Zhang, J.; Manson, J. L.; Miller, J. S. *Adv. Mater.* **1999**, *11*, 914−918. (d) Sokol, J. J.; Hee, A. G.; Long, J. R. *J. Am. Chem. Soc.* **2002**, *124*, 7656−7657. (e) Berlinguette, C. P.; Vaughn, D.; Cañada-Vilalta, C.; Galán-Mascarós, J. R.; Dunbar, K. R. *Angew. Chem., Int. Ed.* **2003**, *42*, 1523−1526. (f) Schelter, E. J.; Prosvirin, A. V.; Dunbar, K. R. *J. Am. Chem. Soc.* **2004**, *126*, 15004−15005. (g) Lescouëzec, R.; Vaissermann, J.; Ruiz-Pérez, C.; Lloret, F.; Carrasco, R.; Julve, M.; Verdaguer, M.; Dromzee, Y.; Gatteschi, D.; Wernsdorfer, W. *Angew. Chem., Int. Ed.* **2003**, *42*, 1483−1486. (h) Wang, S.; Zuo, J. L.; Gao, S.; Song, Y.; Zhou, H. C.; Zhang, Y. Z.; You, X. Z. *J. Am. Chem. Soc.* **2004**, *126*, 8900−8901. (i) Choi, H. J.; Sokol, J. J.; Long, J. R. *Inorg. Chem.* **2004**, *43*, 1606−1608.

(6) (a) Miyasaka, H.; Matsumoto, N.; Ôkawa, H.; Re, N.; Gallo, E.; Floriani, C. *J. Am. Chem. Soc.* **1996**, *118*, 981−994. (b) Miyasaka, H.; Matsumoto, N.; Re, N.; Gallo, E.; Floriani, C. *Inorg. Chem.* **1997**, *36*, 670−676. (c) Miyasaka, H.; Ieda, H.; Matsumoto, N.; Re, N.; Crescenzi, R.; Floriani, C. *Inorg. Chem.* **1998**, *37*, 255−263. (d) Re, N.; Crescenzi, R.; Floriani, C.; Miyasaka, H.; Matsumoto, N. *Inorg. Chem.* **1998**, *37*, 2717−2722. (e) Ferbinteanu, M.; Miyasaka, H.; Wernsdorfer, W.; Nakata, K.; Sugiura, K.-I.; Yamashita, M.; Coulon, C.; Clérac, R. *J. Am. Chem. Soc.* **2005**, *127*, 3090−3099. (f) Miyasaka, H.; Takahashi, H.; Madanbashi, T.; Sugiura, K. J.; Clerac, R.; Nojiri, H. *Inorg. Chem.* **2005**, *44*, 5969−5971.

10.1021/ic060462z CCC: $33.50
Published on Web 08/01/2006

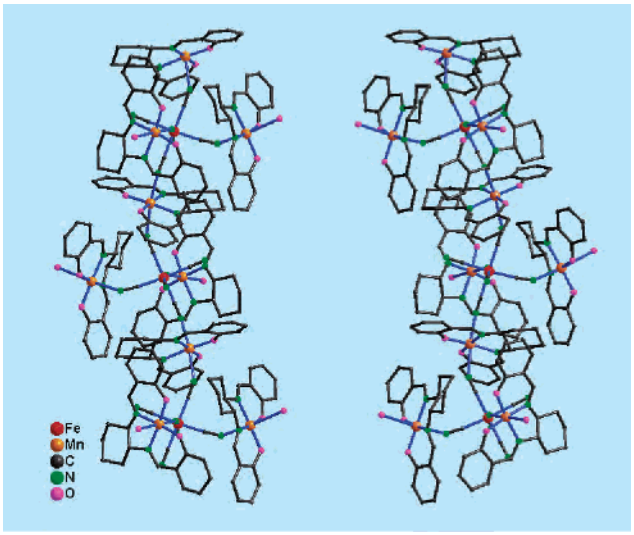

Figure 1. Perspective view of the left- and right-handed helical chains of **1** (*R* isomer, left) and **2** (*S* isomer, right), respectively.

descriptions are presented here for **2**. X-ray structural analyses of **1** and **2** reveal the formation of one-dimensional left-handed and right-handed helical chains, respectively (Figure 1). The left-handed helical chain of **1** consists of the asymmetric chiral unit of $[Mn_3((R,R)\text{-Salcy})_3(H_2O)_2Fe(CN)_6]$ ($FeMn_3$ tetramer) shown in Figure 2. Within the chain, each $[Fe(CN)_6]^{3-}$ unit provides two apical trans cyanide groups to bridge the two $[Mn((R,R)\text{-Salcy})]^+$ units to give a $Mn^{III}-NC-Fe^{III}-CN-Mn^{III}$ uniform chain structure with bond distances of Mn1−N3 [2.398(4) Å] and Mn1#2−N12 [2.251(4) Å] and significantly bent bond angles of C1−N3−Mn1 [148.3(3)°] and C4−N12−Mn1#2 [151.6(3)°] (symmetric operation #2: $-x + 1, y - {}^1/_2, -z + {}^1/_2$) and two equatorial cis cyanide groups to bridge the two $[Mn((R,R)\text{-Salcy})(H_2O)]^+$ units in the terminal mode with bond distances of Mn2−N6 [2.255(4) Å] and Mn3−N9 [2.256(4) Å] and bond angles of C2−N6−Mn2 [143.0(3)°] and C3−N9−Mn3 [152.9(3)°], leaving two cyanide groups free. The Fe−C≡N bond angles in the complex are approximately linear [175.0(3)−179.1(4)°]. The intrachain neighboring Fe···Mn distances are 5.037 and 5.146 Å within the tetramers and 5.175 and 5.284 Å between the tetramers, respectively. There are some short-distance intermolecular interactions between the adjacent chains in the crystal, such as C17−H17···O3 (3.504 Å), C50−H50···C44 (3.705 Å), and C37−H37···C40 (3.449 Å) (Figure S1 in the Supporting Information). The shortest interchain Fe···Fe, Mn···Mn, and Fe···Mn distances are 14.161, 8.314, and 9.251 Å, respectively.

(7) Preparation of complexes **1** and **2**: A solution of $(Bu_4N)_3[Fe(CN)_6]$ (47.0 mg, 0.05 mmol) in acetonitrile (5 mL) was added to a solution of $[Mn((R,R)\text{-Salcy})(H_2O)_2]ClO_4$ (73.6 mg, 0.15 mmol) in 10 mL of acetonitrile. Slow evaporation of the resulting solution in air at room temperature yielded brown-black needle-shaped crystals of **1** after 1 week. Compound **2** was obtained as brown-black needle-shaped crystals in a method similar to that of **1**, except that $[Mn((S,S)\text{-Salcy})(H_2O)_2]ClO_4$ was used. IR (KBr disk): $\nu_{C\equiv N}$ 2119, 2110, and 2026 cm^{-1}. Anal. Calcd (%) for $C_{66}H_{68}FeMn_3N_{12}O_{10}$: C, 56.22; H, 4.86; N, 11.92. Found: C, 56.51; H, 4.69; N, 11.62. Crystal data for **1**: $C_{66}H_{68}FeMn_3N_{12}O_{10}$, $M = 1409.99$, $T = 293$ K, orthorhombic, space group $P2_12_12_1$, $a = 15.279(4)$ Å, $b = 20.027(5)$ Å, $c = 24.285(6)$ Å, $V = 7431(3)$ $Å^3$, $Z = 4$, $\rho_{calcd} = 1.260$ g cm^{-3}, $\mu = 0.749$ mm^{-1}, R1 = 0.0625, wR2 = 0.1247 [$I > 2\sigma(I)$] for 14 499 data and 874 parameters, $S = 1.004$, and Flack $\chi = 0.014(16)$. For **2**: R1 = 0.0583, wR2 = 0.1067 [$I > 2\sigma(I)$] for 14 577 data and 874 parameters, $S = 0.989$, and Flack $\chi = 0.008(14)$.

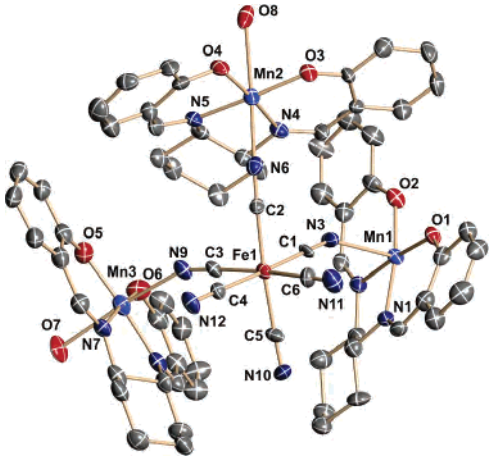

Figure 2. Perspective view of the crystallographically structural unit of **1**. Thermal ellipsoids are set at 30% probability and hydrogen atoms are omitted for clarity. Selected bond lengths (Å) and angles (deg): Mn1−N3 2.398(4), Mn1#2−N12 2.251(4), Mn2−N6 2.255(4), C1−N3 1.159(4), C4−N12 1.145(4), C2−N6 1.176(4), C5−N10 1.127(4); C1−N3−Mn1 148.3(3), C4−N12−Mn1#2 151.6(3), C2−N6−Mn2 143.0(3), C3−N9−Mn3 152.9(3), N3−Mn1−N1 79.69(14), N3−Mn1−O1 87.72(14), N6−Mn2−N4 86.87(14), N6−Mn2−O3 99.01(14), N9−Mn3−N7 89.36(15), N9−Mn3−O5 94.59(16). Symmetric operation #2: $-x + 1, y - {}^1/_2, -z + {}^1/_2$.

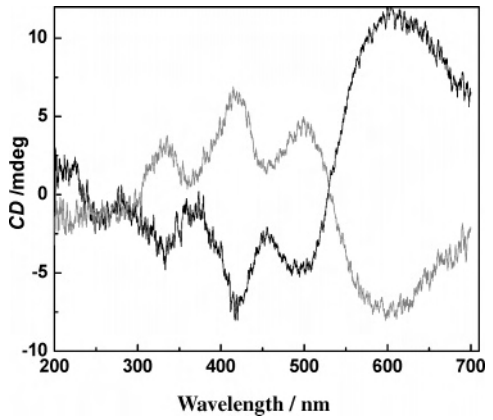

Figure 3. CD spectra of **1** (*R* isomer, black) and **2** (*S* isomer, gray) in KBr pellets.

The circular dichroism (CD) spectrum measurements in KBr pellets further confirm the optical activity and enantiomeric nature of complexes **1** and **2**. The CD spectrum of **1 (***R* isomer**)** exhibits a negative Cotton effect at $\lambda_{max} = 325$, 425, and 500 nm and a positive dichroic signal centered at $\lambda = 600$ nm, while **2** (*S* isomer) shows Cotton effects of the opposite sign at the same wavelengths (Figure 3).

The magnetic measurements were performed on polycrystalline samples of complexes **1** and **2** using a SQUID magnetometer. **1** and **2** show the same magnetic behavior because they are a pair of enantiomers. The temperature dependence of $\chi_M T$ values of **1** is displayed in Figure 4. The $\chi_M T$ value is 9.98 emu K mol^{-1} at 300 K, which is slightly larger than the spin-only value of 9.375 emu K mol^{-1} based on the Mn_3Fe unit ($S_{Mn} = 2$, $S_{Fe} = {}^1/_2$, $g_{Mn} = g_{Fe} = 2.0$). As the temperature decreases, $\chi_M T$ gradually decreases, reaching a minimum value of 2.74 emu K mol^{-1} at 4 K. Upon further

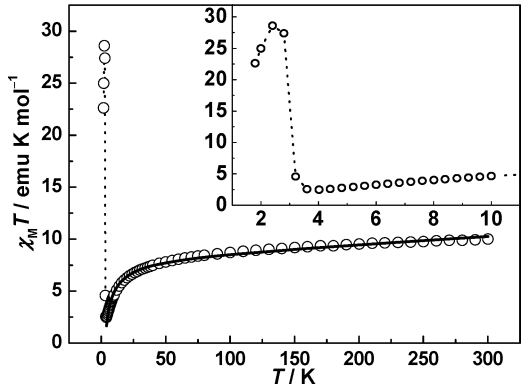

Figure 4. Temperature dependence of $\chi_M T$ for **1** at 100 Oe. The solid line is the fitting from 300 to 4 K, and the dotted line is the guide.

cooling, the $\chi_M T$ value abruptly increases to a maximum value of 28.64 emu K mol^{-1}. This behavior indicates the presence of a ferrimagnetic chain, and antiferromagnetic coupling between Mn^{III} and Fe^{III} ions mediated by cyanide bridges dominates the magnetic properties in **1**. This is confirmed with the fitting results by the Curie−Weiss law. The plot of $1/\chi_M$ vs T (Figure S2 in the Supporting Information) obeys the Curie−Weiss law in the range of 50−300 K with a negative Weiss constant of −21.2(8) K. Based on the structure, **1** can be approximately regarded as a uniform Mn_3Fe chain with the intra- and intertetrameric exchange constants (J and J_c) (see the Supporting Information). The one-dimensional chain model reported previously is used here.[8] The data could be fitted from 300 to 4 K, and the best fit gives the parameters $g = 1.96$, $J = -0.46$ cm^{-1}, $J_c = -0.15$ cm^{-1}, and TIP $= 7.35 \times 10^{-3}$ emu mol^{-1}. The fitting results indicate that cyanide bridges mediate weak intra- and intertetrameric antiferromagnetic coupling between Fe^{III} and Mn^{III} ions. Although both ferro- and antiferromanetic contributions are involved in the magnetic coupling between a high-spin Mn^{III} ($t_{2g}^3e_g^1$) and a low-spin Fe^{III} ($t_{2g}^5e_g^0$), it seems that the antiferromagnetic $t_{2g}-t_{2g}$ ones are dominant in **1**.

At a low applied field of 10 Oe in the temperature range of 1.8−5 K, the magnetizations after zero-field cooling (ZFC) and subsequent field cooling (FC) reveal nonreversibility and bifurcation, confirming the long-range magnetic ordering below 3 K to produce a ferrimagnet (Figure 5). The ac susceptibility measurements in an ac field of 5 Oe oscillating at 1−1500 Hz also indicate a magnetic phase transition occurring at 3 K because the peaks were observed as both in-phase (χ_M') and out-of-phase (χ_M'') around this temperature (Figure S3 in the Supporting Information). The position of the peaks of χ_M' and χ_M'' corresponding to the temperature is not frequency-dependent in the ac measurements, indicating that the single-chain magnetic behavior is not significant in **1**. The field dependence of magnetization shows a gradual increase with the applied field and reaches 6.21 $N\beta$ mol^{-1} at 7 T (Figure 6), which is far from the saturation state

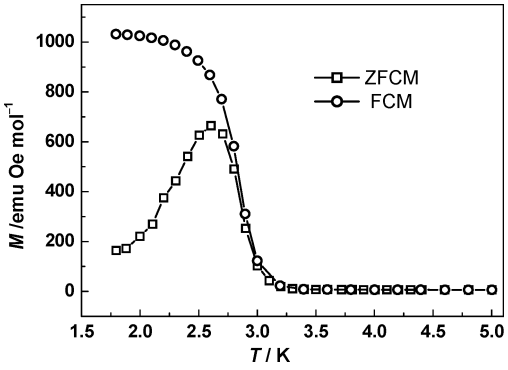

Figure 5. Temperature dependence of magnetization for a polycrystalline sample of **1** at 10 Oe: ZFC (□) and FC (○) magnetization.

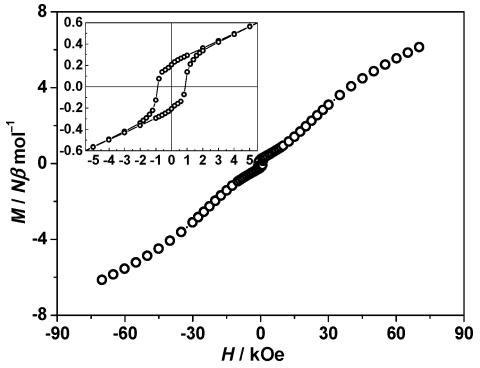

Figure 6. Hysteresis loop at 1.8 K.

compared to the theoretical value of 11 $N\beta$ mol^{-1} ($2 \times 3 \times 2 - 2 \times {}^1/_2$) with the antiferromagnetic coupling between Mn^{II} and Fe^{III} ions. A hysteresis loop with a remnant magnetization of 0.206 $N\beta$ mol^{-1} and a coercive field of 0.87 kOe is observed at 1.8 K, confirming that **1** is a ferrimagnet.

In summary, two enantiomorphous chiral complexes were synthesized, and they are ferrimagnets with the magnetic transition temperature at 3 K. The spin carriers of Mn^{III} and Fe^{III} ions in the helical chain structures may be expected to show a chiral helical nature, which is rare in the literature.[4d] To confirm this possibility, the larger single crystals are necessary in order to measure the spins on the magnetic centers by neutron diffraction. Further investigations on chiral cyano-bridged bimetallic systems with larger dimensionalities or anisotropies are currently underway in our laboratory.

Acknowledgment. This work was supported by the National Natural Science Foundation of China (Grants 20531040 and 90501002). J.-L.Z. thanks the Program for New Century Excellent Talents in University of China (Grant NCET-04-0469). The authors thank the reviewers for their valuable comments and suggestions to improve the manuscript.

Supporting Information Available: Additional characterization data (PDF) and crystallographic data for complexes **1** and **2** in CIF format. This material is available free of charge via the Internet at http://pubs.acs.org.

IC060462Z

(8) Kou, H. Z.; Zhou, B. C.; Liao, D. Z.; Wang, R. J.; Li, Y. *Inorg. Chem.* **2002**, *41*, 6887−6891.